

Control of inclusions dispersion in thermoelectric $\text{In}_2\text{O}_3/\text{In}_2\text{Ge}_2\text{O}_7$ composites

E. Guilmeau, C. Chubilleau, E. Combe, T. Zhou, and D. Bérardan,

Laboratoire CRISMAT, UMR 6508 CNRS-ENSICAEN, 6 Boulevard du Maréchal Juin, 14050 CAEN Cedex, France

Contact author: emmanuel.guilmeau@ensicaen.fr

Abstract

A series of In_2O_3 based nanopowders with germanium doping (from 0 to 10 atom%) have been synthesized by a citrate method. In that way, the $\text{In}_2\text{Ge}_2\text{O}_7$ inclusions in the Ge doped In_2O_3 matrix observed in the sintered compounds are well distributed in comparison to the specimens prepared by a conventional solid state reaction. The electrical and thermal properties have been compared to those measured on conventional materials. Based on these results, the decrease in the lattice thermal conductivity observed in highly Ge doped compounds can be attributed to the presence of inclusions in the Ge doped matrix.

Introduction

Aiming at the discovery of n-type oxide elements for thermoelectric generators, it has been shown recently that Ge-doped In_2O_3 is a very promising thermoelectric oxide material [1]. It was shown that, by doping In_2O_3 with 0.5 at% Ge, this phase becomes semi-metallic instead of semiconducting, and that its conductivity increases by more than one order of magnitude. Moreover, with higher Ge doping levels, excellent thermoelectric properties were achieved with a decrease in the lattice thermal conductivity due to the presence of empty $\text{In}_2\text{Ge}_2\text{O}_7$ spherical inclusions in the Ge-doped In_2O_3 matrix. However, the origin of the lattice thermal conductivity decrease could not be clearly determined since the increasing amount of secondary phases in the material is correlated to a decrease of the geometrical density and an increasing volume of pores. As the formation of spherical inclusions is

probably linked to big GeO_2 agglomerates in the precursor powder, the use of fine nanocrystalline and homogeneous powders synthesized by soft chemistry is expected to avoid the formation of spherical pores. For that purpose, we synthesized nanopowders by a citrate method and studied the thermoelectric properties of the related bulk ceramics.

Experimental

All samples, belonging to the $\text{In}_{2-x}\text{Ge}_x\text{O}_3$ series, were prepared using the citrate reaction route. Starting precursors, $\text{In}(\text{NO}_3)_3 \cdot 5\text{H}_2\text{O}$ (99.99%, Alfa Aesar), GeCl_4 (99.9999%, Alfa Aesar) and citric acid were mixed in a stoichiometric amount $2-x : x : 1$. It should be noted that hexagonal GeO_2 was synthesized from $\text{Ge}(\text{OH})_2$ germanium hydroxide obtained by chemical precipitation of GeCl_4 in contact with water. The solution composed of indium nitrate, GeO_2 and acid citric was kept at 100°C for several hours until the gel formed. This latter is then decomposed at 600°C for 1h to obtain the indium oxide powders. The resulting powders were pressed uniaxially under 300 MPa, using polyvinyl alcohol binder to form parallelepipedic $2 \times 3 \times 12 \text{ mm}^3$ or cylindrical $\varnothing 20 \times 4 \text{ mm}$ samples. Then they were sintered at 1300°C for 48h in air on platinum foils to avoid any contamination from the alumina crucible. X-ray powder diffraction (XRD) was employed for structural characterization using a Philips X'Pert Pro diffractometer with X'Celerator using Cu-K_α radiation in a 2θ range 10° - 90° . The XRD patterns were analyzed using the Rietveld method with the help of the FullProf software. The scanning electron

microscopy (SEM) observations were performed using a FEG Zeiss Supra 55. The electrical conductivity and thermopower were measured simultaneously using a ULVAC-ZEM3 device from 50°C up to 800°C. The thermal conductivity was obtained at 26°C, 300°C, 800°C and 1000°C from the product of the geometrical density, the heat capacity (Netzsch model DSC 404C Pegasus) and the thermal diffusivity (Netzsch model 457 MicroFlash).

Results and discussion

X-ray diffraction pattern, presented in figure 1, confirms the formation of the In_2O_3 phase without any secondary phases after the calcination at 600°C for 1h. The broad diffraction peaks indicate the formation of small particles with an average size of 10 to 20 nm, as shown in the inset of figure 1.

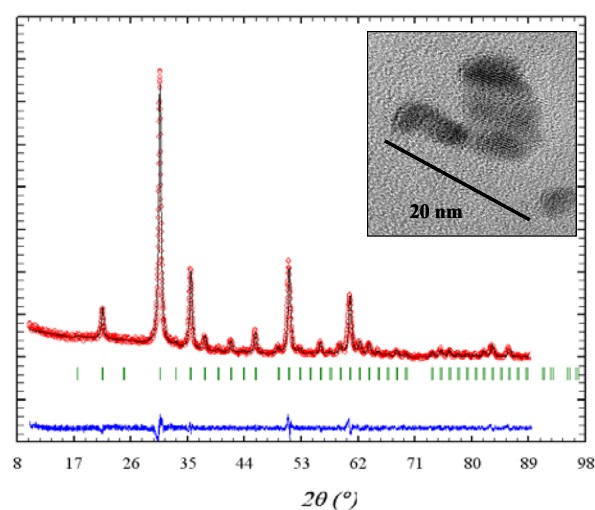


Figure 1: XRD pattern of $\text{In}_{1.99}\text{Ge}_{0.01}\text{O}_3$ calcined powder. Inset: TEM images of particles

The figure 2 presents the XRD patterns of the sintered samples (1300°C/48h) with different Ge contents. Several reflections corresponding to the $\text{In}_2\text{Ge}_2\text{O}_7$ phase for $x \geq 0.01$ suggests a small solubility limit of Ge in the In_2O_3 structure ($x < 0.01$). This result falls in agreement with the previous study on specimens synthesized by conventional solid state reaction (micrometric powders) [1].

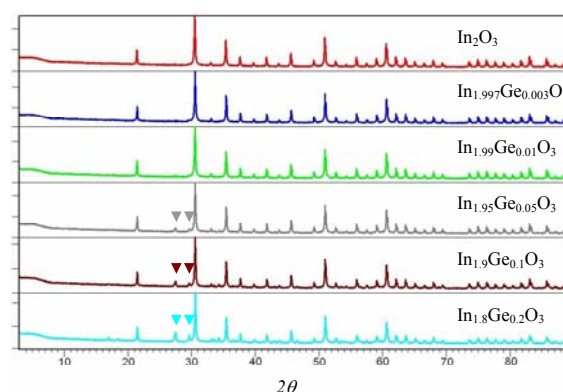


Figure 2: XRD patterns for the samples with different Ge contents.

Figure 3 shows the SEM micrographies of the sintered compounds with different Ge contents. A decrease in the porosity (black zones) can be observed as the Ge content increases up to the solubility limit (as confirmed in figure 4). This phenomenon is correlated to a slight increase of the grains size. The substitution of Ge in the structure (below the solubility limit) promotes the crystalline growth and consequently the material densification. Above the solubility limit, the grain size decreases due to the formation of $\text{In}_2\text{Ge}_2\text{O}_7$ secondary phases which limit the grains growth by diffusion scattering at the grain boundaries. The presence of the secondary phases in the In_2O_3 matrix detectable in the XRD patterns for $x > 0.01$ is also confirmed by SEM observations as shown in figure 3d to 3f (see arrows).

It must be noted that, above the solubility limit, the geometrical density is stabilized to 85% (figure 4). This point is of real importance since it has been shown [2] that the formation of $\text{In}_2\text{Ge}_2\text{O}_7$ spherical inclusions in conventional materials induces a drastic decrease in the geometrical density (figure 4). As expected, the homogeneous and fine nanocrystalline “citrate” powders allow a better distribution of the secondary phases and avoid the formation of sphere pores. This can be clearly observed (figure 5) from the two microstructures of the compounds synthesized by conventional and citrate ways separately, with the same heat treatment (1300°C/48h).

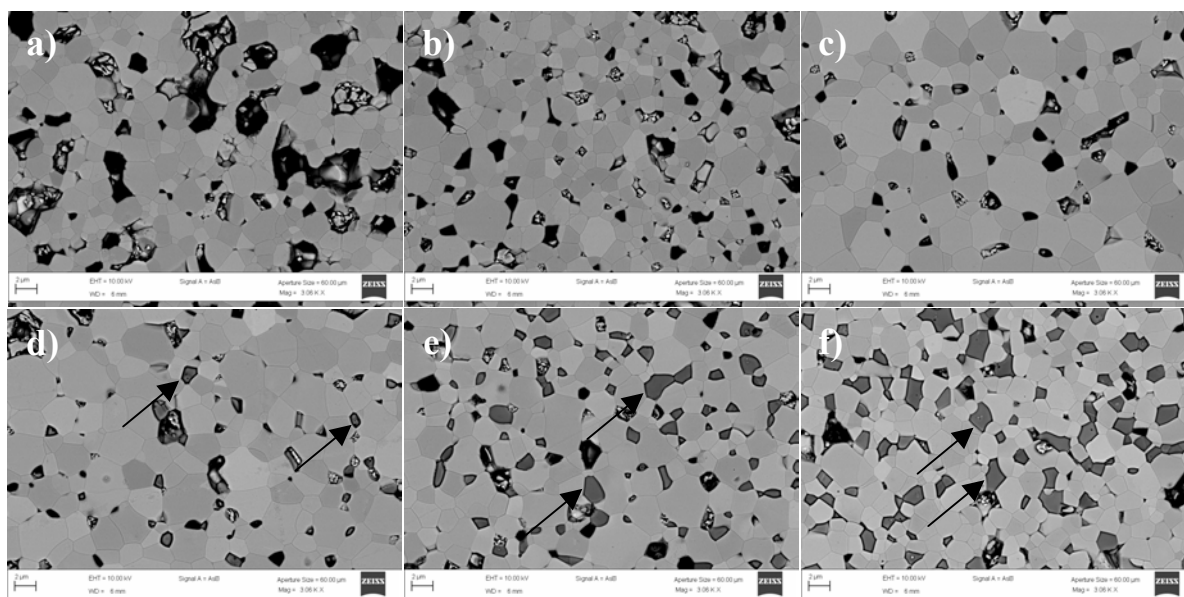


Figure 3: SEM micrographs for the samples with different Ge content. Grey grains correspond to $\text{In}_2\text{Ge}_2\text{O}_7$ inclusions

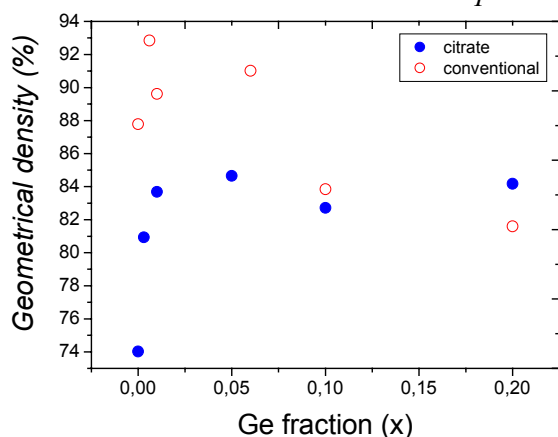


Figure 4: Geometrical densities versus Ge content of samples synthesized from a) conventional and b) citrate method

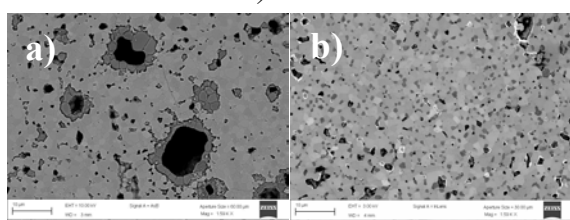


Figure 5: SEM micrographs of $\text{In}_{1.9}\text{Ge}_{0.1}\text{O}_3$ compounds synthesized from a) conventional and b) citrate method

The average grain sizes of the In_2O_3 grains matrix are similar but the distribution and sizes of the secondary phases are different. All samples exhibit a metallic behavior with the electrical resistivity increasing with temperatures (not shown here). The influence of the germanium fraction on the

electrical resistivity at 1000K is shown in figure 6 in comparison with that of samples synthesized from conventional solid state reaction. Both series of compounds exhibit almost the same behavior. Starting from undoped In_2O_3 , a very small addition of germanium, with the order of 0.1 atom% ($x=0.003$), leads to a strong decrease of the electrical resistivity by a factor of 2 or 5, for the citrate and conventional synthesis method, respectively. It is noteworthy that the lower ρ value in undoped In_2O_3 in the case of citrate compounds is presumably linked to a higher oxygen vacancies concentration due to the higher reactivity of the nanocrystalline powders. For both family of compounds, higher doping levels of Ge lead to a decrease of the resistivity with a minimum value of $\rho \sim 1.5 \text{ m}\Omega\cdot\text{cm}$ at 1000K for $x=0.01$. It is noteworthy that this value is very close to the best conductivities observed in bulk In_2O_3 based compounds ([3] and ref. therein). Further additions lead to a slow increase of the resistivity. Therefore, we can propose that the solubility limit for Ge in In_2O_3 may be close to $x=0.01$ and that there is most probably a doping effect due to the substitution of $\text{Ge}(+\text{IV})$ for $\text{In}(+\text{III})$ which would result in an increase of the electrons concentration in the system.

The behavior of the thermopower is

in a similar way (Fig. 6). Starting from undoped In_2O_3 with $S \sim -225 \mu\text{V.K}^{-1}$ at 1000K, a very small amount of ge doping leads to a decrease in the thermopower, which reaches a constant value $S \sim -110 \mu\text{V.K}^{-1}$ when the germanium fraction exceeds $x=0.01$. From these results, we can conclude that the precursors and consequently the dispersion of secondary phases in the slightly Ge doped In_2O_3 matrix have little influence on the electrical transport properties. The Ge doping level in the In_2O_3 structure is therefore predominant on the power factor in the present range of secondary phases content.

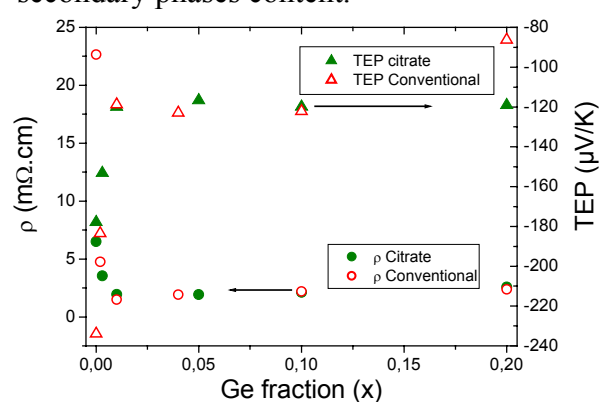


Figure 6: Influence of the germanium fraction (x) on the electrical resistivity.

Finally, the figure 7 shows the variation of ZT according to the Ge fraction for both compounds families. Almost similar values were obtained, except for undoped In_2O_3 which exhibits a $ZT=0.37$ in the case of citrate compounds, related to the lower electrical resistivity values as discussed above. The most interesting point remains the evolution of the λ_e/λ_L ratio versus Ge content as shown in the inset of figure 7. For “conventional” compounds, it has already been reported [1] that the first increase of λ_e/λ_L for low germanium fractions is mainly linked to the decrease of the electrical resistivity. The ratio exhibits a local maximum for a germanium fraction that corresponds to the solubility limit. However, it is noteworthy that λ_e/λ_L increases as x increases for high germanium fractions, although the electrical conductivity (and therefore λ_e) decreases.

As the presence of $\text{In}_2\text{Ge}_2\text{O}_7$ and the increase of porosity due to the empty spherical agglomerates formation in conventional compounds are highly correlated, it is not possible to determine whether this effect on the thermal conductivity mainly originates from the inclusions or from the pores. In the present study, since the citrate compounds show well distributed $\text{In}_2\text{Ge}_2\text{O}_7$ inclusions and exhibit same densities, it can be established that the presence of inclusions may contribute to a the decrease in the lattice thermal conductivity. This point is of importance with the aim to develop new thermoelectric composites.

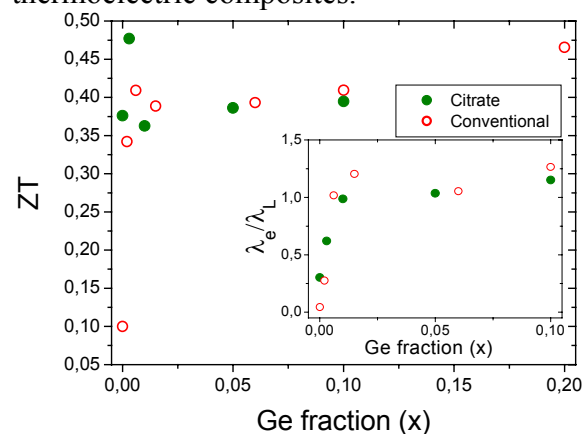


Figure 7: Calculated dimensionless figure of merit ZT as a function of the germanium fraction. The inset shows the ratio of the electronic part to the lattice part of the total thermal conductivity at 1273K as a function of the germanium fraction.

Conclusion

The controlled dispersion of $\text{In}_2\text{Ge}_2\text{O}_7$ inclusion in the Ge doped In_2O_3 matrix through the citrate method leads to electrical and thermal properties comparable to those measured on conventional materials. More especially, the homogeneous dispersion of the inclusions may contribute to a decrease in the lattice thermal conductivity.

References:

- [1] D. Bérardan, E. Guilmeau, A. Maignan, and B. Raveau, *Solid State Comm.* **146** (2008) 97.
- [2] D. Bérardan, E. Guilmeau, A. Maignan, and B. Raveau, *Proceeding IEEE, ICACC 2008*, to be published.
- [3] L. Bizo, J. Choynet, R. Retoux, and B. Raveau, *Solid State Comm.* **136** (2005) 163.